Journal of Porous Materials (2021) 28:853–865
https://doi.org/10.1007/s10934-021-01037-9

Synthesis and characterization of cryogels of p(HEMA-N-vinylformamide) and p(HEMA-N-Vinylpyrrolidone) for chemical release behaviour

Koray Şarkaya[1] · **Abdulkadir Allı**[1]

Accepted: 20 January 2021 / Published online: 3 February 2021

Abstract
Macroporous polymeric gels has received great attention in many fields focused on biotechnological applications. In this study, two new HEMA-based cryogel columns were synthesized. To this end, poly(HEMA-VF) and poly(HEMA-NVP) cryogels were prepared by copolymerization of 2-Hydroxyethyl methacrylate (HEMA) with N-vinylformamide (VF) and N-vinylpyrrolidone (VP) in the presence of N,N-methylenebisacrylamide (as cross-linker), then polymerization initiated by ammonium persulfate (APS) and N,N,N′,N′-tetramethylenediamine (TEMED) with free-radical polymerizations method in cryogelation conditions, respectively. p(HEMA-VF) and p(HEMA-VP) cryogels contain a continuous polymeric matrix with interconnected pores of size 2–100 µm. Swelling behavior for these cryogels in various solvents was investigated, wherein the characterization of the cryogels is conducted via by surface area measurement (BET), Fourier transforms infrared spectroscopy (FT-IR), elemental analysis, scanning electron microscopy (SEM), Differential Scanning Calorimetry (DSC) and Thermogravimetric Analysis (TGA). As drug model compounds, Methyl Red (MR), methylene blue (MB) and methylene green (MG) were loaded into prepared cryogels and the controlled release properties of cryogel columns were examined comparatively each other. It has been shown that approximately 90% of its release from the cryogels occurred within about 2 h. In addition, MB release from p(HEMA-VF) and p(HEMA-VP) cryogels was found to be around 80% over a similar period. The proposed cryogels can be regarded as controlled release system on future biomedical applications.

Keywords Drug delivery systems · N-vinylformamide (VF) · N-vinylpyrrolidone (VP) · Supermacroporous cryogel

1 Introduction

In terms of biotechnological applications, macroporous gels have always been of interest from for the last two decades [1, 2]. Hydrogels are three-dimensional cross-linked hydrophilic polymeric networks that can maintain their physical structure even under various environmental conditions such as pH, heat, electric field and ionic strength and can swell up to hundreds of times their original size with the absorbing water ability, also considered as an intermediate between liquids and solids [3]. They are important functional materials that have numerous potential applications thanks to their inherent characteristics, e.g. flexibility and elasticity, and are used in the design of advanced materials [4]. Cryogelation is a simple method to prepare durable macroporous gels that respond quickly to stimulants. The polymerization starts in a frozen water-soluble monomer/polymer mixture, where cryogelation occurs in the interstitial spaces between the ice crystals. After the thawing of ice crystals, which are the pore-forming functional component, a polymer network consisting of interconnected pores is formed [5]. The advantages of cryogelation in the preparation of hydrogels are that ice crystals play the role of inert templates, thus avoiding the absence of any organic porogen [6]. Cryogels are referred to be as three-dimensional magaporous hydrogel matrices that can be synthesized by the method of free radical polymerization at a temperature below the freezing point of the solvent, usually using an initiator/activator system, by photo or electron-beam initiation [7]. Unlike conventional hydrogels, cryogels have large pore size, short diffusion path, good biocompatibility, and high mechanical and physical stability [8]. For example, the fact that cryogel production

✉ Koray Şarkaya
koraysarkaya@duzce.edu.tr

[1] Department of Chemistry, Duzce University, 81620 Düzce, Turkey

takes place at temperatures below zero degrees protects the proteins from conformational changes, and since natural ice crystals are used instead of harmful organic solvents as pore builders, health-damaging situations in the purification and transport of food and therapeutic agents are minimized [9, 10]. Cryogels can be synthesized from a variety of artificial and natural polymers or combinations thereof. In addition, these materials may be formed by both physical and chemical crosslinking of polymeric networks. It is also prepared from water-soluble monomers with excellent chemical and biological stability. Water-soluble monomers containing functional groups can easily polymerize with suitable crosslinking agents. For example, such as hydroxyethyl methacrylate (HEMA) [11], acrylamide (AAm) [12], N-isopropylacrylamide (NIPAm) [13], dimethacrylamide (DMAAm) [14], Hydroxypropyl methacrylate (HPMA) [15], N,N-dimethylaminoethyl methacrylate (DMAEM) [16] are among the most commonly used monomers for this purpose. Due to its properties based on mechanical and thermal stability, also with biocompatibility on synthesis process, 2-hydroxyethyl methacrylate (HEMA)-based cryogel and it's modifications are frequently used in many applications still in literature [17–20]. Cryogels that can be produced in monolithic column, membrane-disk, spherical or micro-shape have a wide range of applications covering the fields of insulation, environment, food, health, biotechnology, catalytic reduction of organic compounds and electronic approaches, recently [21–23]. For example, these polymeric materials can be used efficiently in biosensors [24], as support material in chromatography [25], tissue scaffold in tissue engineering [26], therapeutic agent delivery system such as drug or protein [27]. In addition, cryogels can be produced as exclusive composite materials prepared by increasing the surface area by embedding micro- or nano scale spheres, beads or gels in the cryogel matrix [28]. Also, cryogels are unique because they are prepared by a very simple method, allowing the formation of interconnected large open pore network structures that can participate in a wide variety of applications depending on the it's morphological features [29]. Cryogels are known as mezoporous or macroporous gels, have spongy morphology. It has thin polymeric walls, usually non-porous, and large continuously interconnected pores. These interconnected macropores allow mobile phase flow with negligible flow resistance. Parametres are such as the concentrations of both monomer and cross-linker primarily used in the polymerization reaction, the ionic strength and pH of the solution, the change in the cooling rate of the polymerization cryogelation conditions cause differences in the pore size and pore wall thickness differentiation of cryogels. The size of macropores in cryogels ranges from tens or even hundreds to just a few micrometers. Pores of the cryogels acts as the channel for the easy diffusion of drug molecules into polymer, and then the pore size, pH and / or temperature of ambient conditions control the release of the drug entrapped in the cryogels. This exclusive feature makes it important for potential applications of cryogels in drug-controlled release systems [30–33]. In addition, there are studies in the literature for various azo dyes, whose adsorption are quite predictable due to their intense color, are also can be used as model test drugs in oerder to investigation for the release performance of hydrogels [34–37].

In this study, the free radical polymerization method was applied and the N-vinylformamide (VF) and N-vinylpyrrolidone (VP) monomers were copolymerized with HEMA, then p(HEMA-VF) and p(HEMA-VP) cryogels were synthesized for the first time in the literature. N-vinylformamide (VF) is a water-soluble, colorless liquid, which dissolves in most polar solvents, such as methanol, ethanol, chloroform, and THF. N-Hexane and n-butane are two of its poor solvents. VF is stable and can be stored at room temperature for months. VF has shown attractive high reactivities in polymerization, copolymerization, and hydrolysis, and it was selected as the comonomer since it is water-soluble and possesses much lower toxicity than acrylamide [38]. Also, having good solubility in water and in some organic solvents, N-vinylpyrrolidone (VP) is one of the hydrophilic monomers suitable for the synthesis of hydrogels but also provides the use as a dressing material [39]. Although VF and VP based hydrogel synthesis are encountered within the scope of the literature review [40–44], studies about, which two monomers are subjected to copolymerization in cryogel form are quite limited [45]. As mentioned, the main criterias for choosing p(HEMA) as the main monomer are inert, mechanical resistance, chemical, and biological stability features of the monomer. The swelling behavior of cryogels in some of polar and non-polar solvents was investigated. FT-IR, SEM, BET, Elemental, DSC, and TGA analyzes were performed for the characterization of the prepared cryogels. Dyes of methyl red (MR), methylene blue (MB) and methylene green (MG) was selected as the drug model to investigation of release performances of cryogels. Kinetic and isotherm calculations were performed depending on release studies.

2 Experimental section

2.1 Materials

The monomers HEMA (2-Hydroxyethyl methacrylate), VF (N-vinylformamide) and VP (N-vinylpyrrolidone), and [(N, N'-methylene-bis(acrylamide)), (MBAAm)] as cross-linker were obtained from Sigma (Sigma Chemical Co., USA). Ammonium persulfate (APS) as an initiator and N,N,N',N'-tetramethylene diamine (TEMED) as the accelerator was obtained from Fluka A.G. (Buchs, Switzerland). All dyes

were obtained from Merck AG, Germany. The other materials used in the experiments were of chemical purity and were washed with distilled water. Buffer and sample solutions were filtered before use with a 0.2-µm membrane (Sartorius, Göttingen, Germany). Before starting the experiments, all glassware was washed with the dilute nitric acid solution.

2.2 Synthesis of cryogels

The procedure of the HEMA-based cryogel sample is mentioned before previous studies [11, 46]. Accordingly, with procedure for this study, 1.3 ml of HEMA and a 170 µl of NVF were dissolved in 5 mL water, and 0.2 g of MBAAm was dissolved in 10 mL water. Then, these two solutions mixed together. 20 mg APS was added to the mixture and it was dissolved thoroughly. Subsequently, 25 µL of TEMED was added, and after mixing, the solution was dispensed into 5 mL plastic syringes (0.8 cm in diameter). Cryogel solutions were quickly cooled to -18 °C and kept at this temperature for 24 h. The cryogel, which is produced by free-radical polymerization, was removed from the freezer after 24 h. Prepared cryogel was washed with distilled water for several hours, in case there may be unreacted monomers. The same procedure above was used for the synthesis of p(HEMA-NVP) cryogel with the addition of a 210 µl of NVP, instead of NVF monomer. In order for the results to be comparable, p(HEMA) cryogel was synthesized. The preparation of pure p(HEMA) cryogel does not include the both N-VF and N-VP monomers in the procedure mentioned.

2.3 Swelling and porosity tests of cryogels

All cryogel samples were dried at 50 °C. Dried cryogels were weighed, then placed in 50 ml of distilled water and kept in water for 2 h. The interaction of the cryogels with water was terminated, then it was wiped from a filter paper and its weight was measured again. Qualitative results for all cryogels weights was taken both in the dry state and in the water. As shown in the following Equation (Eq) (1) expression, the quantitative difference between the weights of the cryogel in both cases allowed determination of the water uptake rate of the cryogels. The scope of this test was expanded by using solvents such as n-hexane, benzene, ethanol, acetone, chloroform, methanol, N,N-dimethylformamide (DMF), acetonitrile, and dimethyl sulphoxide (DMSO) as non-polar or polar ones to investigate the swelling ability of cryogels. The swelling degree of cryogels was defined as:

$$\text{The solvent uptakeratio } \% = [(W_s - W_0)/W_0] \times 100 \quad (1)$$

W_o is the weight of the cryogel before swelling and W_s is the weight of the cryogel after swelling.

The total volume of macropores in the swollen cryogel was roughly estimated by the weighing sample ($W_{squeezed\ gel}$) after squeezing free water from the swollen gel matrix. The % porosity was calculated as [15, 47];

$$\text{Porosity } (\Phi)\ \% = [(W_s - W_{squezzed\ gel})/W_s] \times 100 \quad (2)$$

$$\text{Gelling efficiency } \% = [(W_0/W_t)] \times 100 \quad (3)$$

According to this equation w_t; refers to the total mass of monomers in the polymer syrup.

2.4 Characterization studies

The structure of p(HEMA), p(HEMA-VF) and p(HEMA-VP) cryogels was examined by FTIR Spectrometer (Thermo Nicolet iS10 FTIR-ATR Spectrometer, USA) was taken in the wavelength range 400–4000 cm^{-1} to investigate whether N-vinylformamide and N-vinylpyrrolidone are added to the structure of p(HEMA)-based cryogels that are intended to be functional with VF and VP, then the results obtained were compared with each other. Before analysis, the samples were dried in the oven at 50 °C for 6 h. The surface area and porosity properties of cryogels were determined by using the Brauer-Emmett-Teller (BET) method with mercury porosimetry. The surface morphology of prepared cryogels was examined using SEM (Carl Zeiss AG—EVO® 50 Series, Germany). For the preparation protocol of samples for SEM analysis, a dried cryogel sample was attached to the SEM holder with double-sided carbon tape before coating with a thin layer of gold under vacuum. Then, cryogel sample was placed into the SEM instrument and images were taken at different magnification rates. The elemental analyzer (Flash 2000 CHNS/O Analyzers, USA) was used to determine the content of the obtained cryogels. 10 mg of polymer sample was weighed with precise sensitivity into the cell of the elemental analyzer and as a result of the combustion process, the percentage of carbon (C), hydrogen (H), and nitrogen (N) was determined as the polymer sample. The thermogravimetric analyzer (Shimadzu DTG-60H, Japan) was used for the determination of the chemical content and thermostability of cryogels. In that case, the temperature increment and nitrogen flow rate were, respectively, set to 10 degrees/min and 100 mL/min.

2.5 Dye loading and release studies

In this study, the release performances of cryogels were investigated using methyl red (MR), methylene green (MG), and methylene blue (MB) as model drugs. The experimental method was carried out according to the procedure in the literature [34]. All dried cryogels were left to swell for one day at 25 ^{0}C in beakers containing 100 ppm (mg/L) methyl red,

methylene blue, and methylene green solution prepared in an aqueous solution. The cryogels left to swell in the prepared dye solutions were removed from the solution the next day and the dye residues remaining on the surface of the cryogels were dried with towel papers. The dye loaded-cryogels were dropped into 50 mL of distilled water and chemical release was initiated. The absorbance values of the aqueous dye solutions released from the sample were measured on a UV–VIS spectrometer. Absorption values of the dye solutions was measured at 440 nm, 668 nm and 633 nm wavelengths for MR, MB, and MG, respectively. The standard calibration curves of the absorbance as a function of the MR (at 440 nm), MB (at 668 nm), and MG (at 633 nm) has a linear relationship with correlation coefficients (r) of 0.9934, 0.9991, and 0.9967, respectively. Dye concentrations in solutions released from the cryogels was calculated as a result of the equation derived from the absorbance data obtained from the calibration curve.

This linear relationships can be measured by the following equations:

$$y = 0.0002x + 0.0063 \,(\text{for MR, at } 440\,\text{nm}),$$

$$y = 0.2308x + 0.0326 \,(\text{for MB, at } 668\,\text{nm})$$

$$y = 0.1921x + 0.0632 \,(\text{for MG, at } 633\,\text{nm})$$

Dye concentrations in solutions released from the cryogels was calculated as a result of the equation derived from the absorbance data obtained from the calibration curve. In swellable systems, drug release usually occurs under conditions that are incompatible with Higuchi or Fickian behavior. The following equation can be written for diffusion-controlled and swelling-relaxed controlled drug release [48].

$$\frac{M_t}{M_\infty} = k_1\sqrt{t} + k_2 t \tag{4}$$

Equation (4); denotes constants k_1, k_2 and m. The first term to the right of equality refers to Fickian diffusion (F) and the second term to Case-II transport (R). This equation can be written more generally as follows:

$$\frac{M_t}{M_\infty} = kt^n \tag{5}$$

In this equation; the total amount at the time of m_t, t; M_∞ is the total amount when it reaches equilibrium; k is the constant associated with the geometric characteristics of the system; n refers to the release exponent, which indicates the drug release mechanism.

This equation was first reported in 1985 by Peppas et al. Therefore, it is also known as "Peppas equation". Peppas equation is valid for the first 60% release [49]. The drug release mechanisms and the values of the release exponent are shown in Table 1.

3 Results and discussion

3.1 Characterization results

All prepared cryogel columns are cylindrical shape, and also have opaque, spongy, and elastic structural properties. One of the most typical features of cryogels is the interconnection of macropores and spongy morphological structures. Most of the water contained in spongy cryogels is in macropores and can be removed from macropores by mechanical compression. When the cryogels that have shrunk by losing their water are kept in the water again, they regain their original size and appearance in a short time. Drying and re-inflation can be repeated without damaging the macroporous structures of the cryogels. Therefore, these properties provide a good advantage for chromatographic applications of these macroporous polymers. Optical photographs for the morphological size of both p(HEMA-VP) and p(HEMA-VF) cryogels are given in Figs. 1a and b, respectively.

The elemental composition of p(HEMA), p(HEMA-VF), and p(HEMA-VP) cryogels was measured by the EDAX method. Also, element mapping for all cryogel samples was shown by the same method in between Fig. 2a and c. The mass percentage of elements for these cryogels were 53.86% C (carbon) and 46.14% O (oxygen) for p(HEMA)-based cryogels, 45.04% O, 49.04% C, and 5.92% N for p(HEMA-VF) cryogel, 44.12% O, 48.27% C, and 7.61% N for p(HEMA-VP) cryogel, respectively. This indicates the presence of ''N'' atoms in the VF and VP monomer. Because of the presence of these atoms, this monomer can be evaluated as a co-monomer. It can also be regarded as a functional monomer by allowing coordinated covalent bonds to be made over

Table 1 Drug release mechanisms and the values of the release exponent

n, release exponent			Drug release mechanism
Thin film	Cylinder	Sphere	
0.5	0.45	0.43	Fickian diffusion
$0.5 < n < 1.0$	$0.45 < n < 0.89$	$0.43 < n < 0.85$	(Non-Fickian) Anamalous transport
1.0	0.89	0.85	Case-II transport

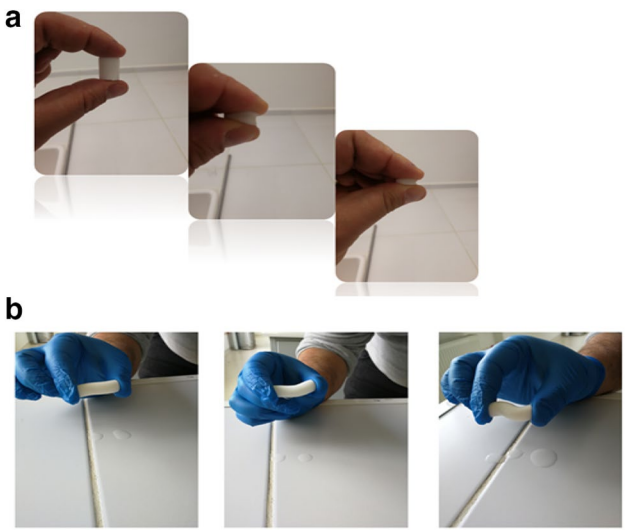

Fig. 1 Elastic morphology of cryogel samples; **a** p(HEMA-VP) cryogels, **b** p(HEMA-VF) cryogels (Color figure online)

the nitrogen groups with the metal groups as template ions for future studies based on molecularly-imprinted polymers.

The ability of the functional groups to characterize the incorporation of N-vinylformamide and N-vinylpyrrolidone monomers into PHEMA cryogel was determined by FTIR spectrophotometry. The changes that occur after the monomers have been incorporated into cryogels are shown in Fig. 3 of the cryogels and can be examined in the FT-IR spectra. FTIR spectrum of poly (HEMA) cryogel is shown in Fig. 4. When the spectrum is examined, there are 3300 cm^{-1} (OH stretch), 2960 cm^{-1} (CH alkyl stretch), 1710 cm^{-1} (C = O stretch) and 1150 cm^{-1} (C-O stretch) bands. When the spectra are evaluated together, many common bands are seen. Similar bands in the spectrum of the p(HEMA) cryogel are also found in the spectrum of the p(HEMA-VF) cryogel, but addition for p(HEMA-VF) cryogels; the peaks around 3200–3350 cm^{-1} have characteristic N–H vibration bands and these peaks are observed together since the -OH group is present in the structure. The peak observed around 1244.09 cm^{-1} belongs to the C-N vibrations. The peaks are at 1653 cm^{-1} and 1530 cm^{-1} indicates the Amide I and Amide II bonds, respectively. Also, the FT-IR spectra of N-vinylpyrolidone HEMA-based cryogel is examined, it is observed at 3385 cm^{-1} (O–H stretching), 2942 cm^{-1} (aliphatic streches), 1724 cm^{-1} and 1658 cm^{-1} (C = O stretching, ester carbonyl, the most significant observation is the polymerization rate of the band at 1658 cm^{-1} compared to the characteristic band of the groups of carbonyl and amide, respectively) and 1426 cm^{-1} and 1152 cm^{-1} (C–O–C bending and C-N stretching). In all HEMA-based cryogel synthesis, it has been registered that HEMA is fully involved in the structure.

The Surface and bulk structure of cryogels were examined by scanning electron microscopy (SEM). For this purpose, the polymer part was attached to the SEM sample plate with a conductive adhesive. Subsequently, the sample surfaces were covered with 200 Å thick metallic gold under vacuum to make the surface conductive. Prepared samples were placed into SEM sample chamber and photographed at various magnification rates. Ice crystals form during the polymerization of cryogels, and when ice crystals melt, interconnected pores are formed. In Fig. 4, SEM photographs of p(HEMA), p(HEMA-VF) and p(HEMA-VP) cryogels are shown. An advantage of cryogels is that the pores inside are large, so the contact surface is lower than expected. As can be seen from SEM photographs for all

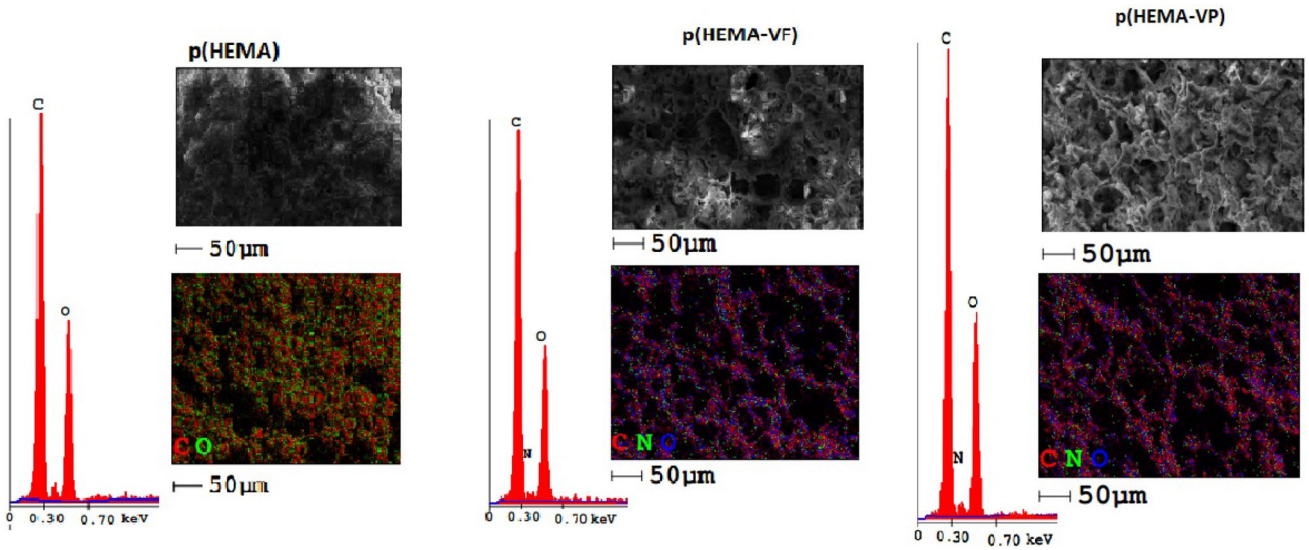

Fig. 2 Elemental analysis results and elemental mapping for cryogels **a** p(HEMA), **b** p(HEMA-VF) and **c** p(HEMA-VP) cryogels (Color figure online)

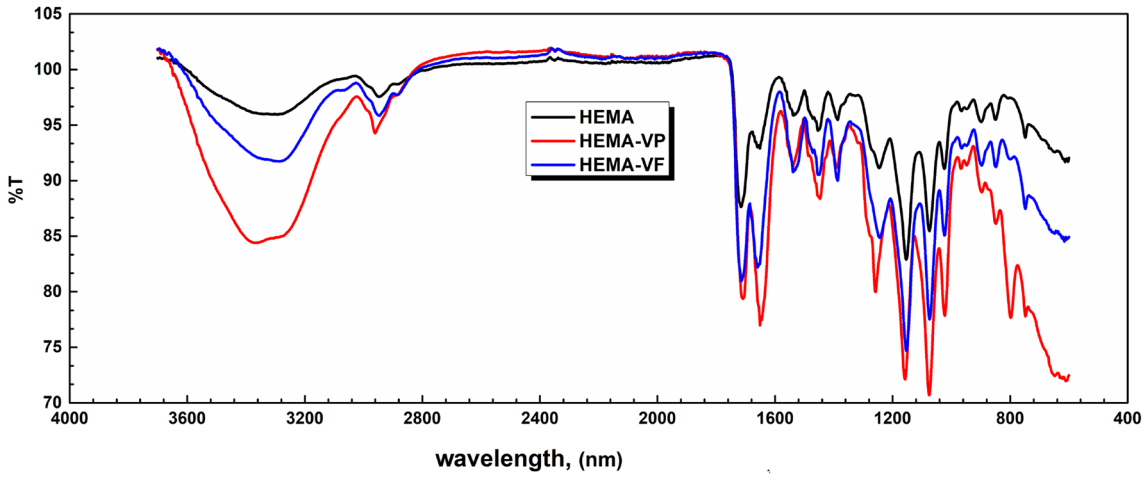

Fig. 3 FT-IR spectrums of p(HEMA), p(HEMA-VF) and p(HEMA-VP) cryogels (Color figure online)

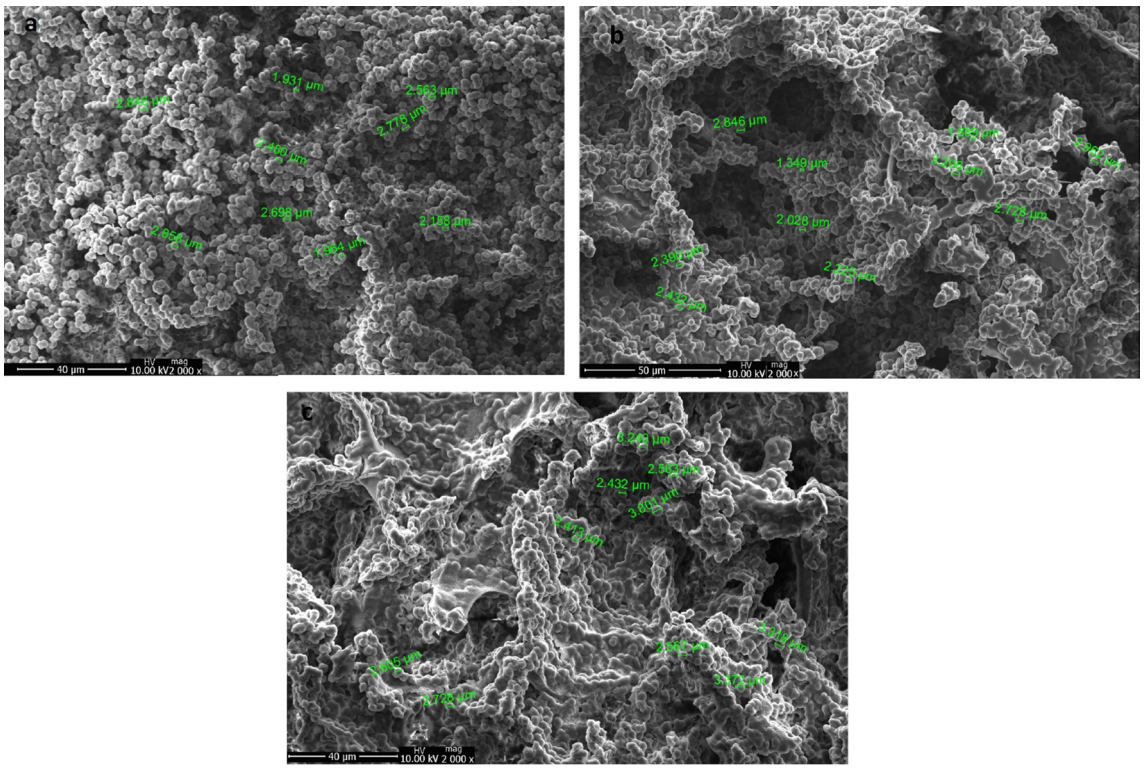

Fig. 4 SEM photos of cryogels; a: p(HEMA), b: p(HEMA-VF) and c: p(HEMA-VP) (Color figure online)

HEMA-based cryogels, the pores are in the range of approximately 2–100 µm. It is clearly seen from the SEM photographs that the all cryogel structures has a porous structure, interconnected porous channels and homogeneously cross-linked network structure. It is also observed that there are no smooth fractures in its morphological structure that impair the structural integrity. This situation is consistent with the results of swelling tests and has been evaluated as evidence that cryogels can maintain their structural stability longer during the experiments. Thanks to the wide pores, when working with viscous liquids such as tissue extract and blood, there is no back-pressure problem in the cryogel columns. Thus, there is no diffusion restriction and mass transfer is easier compared to conventional columns containing microspheres. The pore size of the matrix is much larger than the size of the biomolecules (protein or drugs

etc.) or organic compounds as dyes, which allows them to pass easily. As a result of the convective flow of the solution through the pores, the mass transfer resistance can be practically neglected. This open structure allows the liquid to be forced from the polymer without being compressed using flow rates of the polymer suitable for chromatographic purposes [50]. In addition, this situation provides a suitable ground for adsorption studies. According to the results of surface area measurements performed with mercury porosimetry, the surface areas of p(HEMA), p(HEMA-VF) and p(HEMA-VP) cryogels are 15.31 m^2/g and 16.99 m^2/g and 16.42 m^2/g, respectively. Pore size distributions are determined by mercury porosimetry, so for all cryogel columns pore sizes are in the range of 2–100 µm. It is seen that the results of SEM photographs and mercury porosimetry are compatible with each other. Inferring from these results that cryogels were successfully synthesized, and the pore size and distribution were as expected.

TGA method was used to examine the thermal stability and chemical content of p(HEMA), p(HEMA-VF) and p(HEMA-VP) cryogels. Also, a thermogram of p(HEMA) cryogel was investigated with the same process, so that comparison of the results with other cryogels. To meet the requirements of this method, weights of cryogels were recorded at different temperatures and the results are shown in Fig. 5a. When we examine the thermogram of p(HEMA-VF) cryogel, it is understanding that there are two thermal degradations. The majority of mass loss occurs after the first thermal degradation. The mass loss after the first degradation that started after 270 °C is around 73.48%. After 370 °C, the second thermal degradation started and with its 90.61% mass loss, its thermal stability continues up to 650 ^{0}C due to its cross-linked natural structure. According to the thermogram of p(HEMA-VP) cryogel, the first thermal degradation started just above 300 °C. Approximately 69.05% of the mass loss is experienced in this process. At almost 400 °C, this time the second thermal degradation takes place, and the mass loss reaches about 89%. The thermal stability of this cryogel continues just above 650 °C due to the presence of its cross-linked structure. Two thermal degradations are observed in the thermal analysis of pure p(HEMA) cryogel. These results are consistent with studies in the literature for pure p(HEMA) cryogel [51, 52]. The onset temperatures of these mass losses are observed at earlier temperature points

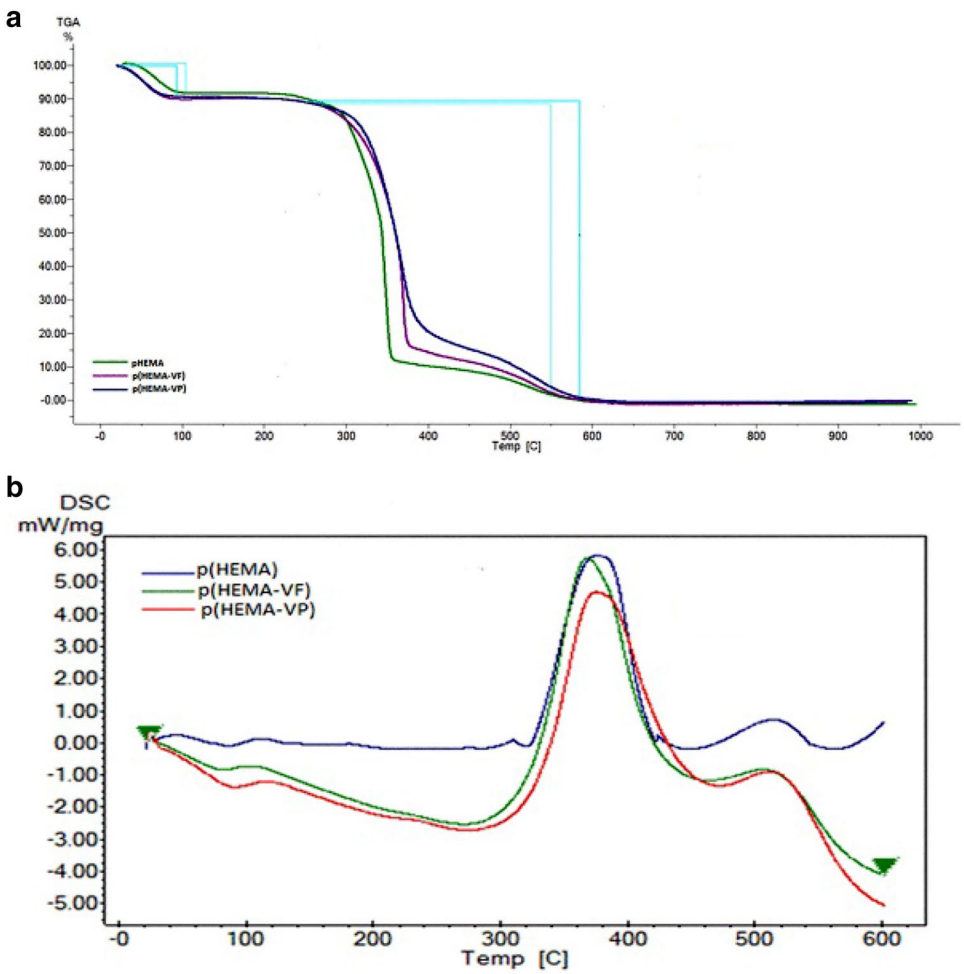

Fig. 5 **a** TGA thermograms of p(HEMA), p(HEMA-VF) and p(HEMA-VP) cryogels. **b** DSC thermograms of pHEMA, p(HEMA-VF) and p(HEMA-VP) cryogels (Color figure online)

compared to the corresponding values of p(HEMA-VF) and p(HEMA-VP) cryogels, while thermal stability ends at around 610 °C. It can be interpreted that the thermal stability of the new crosslinked cryogels obtained as a result of copolymerization of the HEMA monomer with N-NF and N-VP monomers is longer, the mass losses are more delayed, and the presences of comonomers increase the thermal stability of HEMA-based pure cryogels. One of the common behaviors in all cryogel samples is the observation of mass loss in and around 100 °C of temperature. It is thought that this situation may still have some water residue in every structure.

When the sample undergoes a physical or chemical change, a change due to these changes is observed in the enthalpy. The amount of energy absorbed or released while the sample is being heated, cooled, or maintained at a constant temperature is measured by a differential scanning calorimetry device (DSC). DSC thermograms were obtained to analyze the thermal behavior of the prepared cryogels. Also, Fig. 5b shows the DSC thermograms of cryogels. The glass transition temperature (Tg) was found at 80 °C during the first transition in the DSC curve for pHEMA cryogel. And, thermogram also shows a sharp endotherm starting at 336 °C and ending at about 410 °C with a peak at 380.19 °C, which simultaneously represents the melting point (T) and degradation of the PHEMA cryogel. Depending on the synthesis conditions, it can be understood from the similar analyzes in the literature that the glass transition temperatures of pure p(HEMA) cryogels can occur between 80–100 °C [53]. Regardless of temperature and independent of gamma radiation, the value for (Tg) of obtained pHEMA cryogel after bulk polymerization is 80 °C. The initial endothermic transition temperature for p(HEMA-VP) cryogel is observed to be about 90 °C, which corresponds to the initial (Tg_1) temperature. And, melting point and decomposition temperature (Td) are determined from the second endotherm observed from 298 °C to 410 °C with a peak value centered at 368.29 °C. For p(HEMA-VP), Tg_1 was determined as 90 °C. Then, with the peak at 375 °C, melting point and decomposition temperatures can be observed again from the second endotherm curve range of 320 – 420 °C.

(The glass transition temperature (Tg) and decomposition temperatures (Td) data for all cryogels obtained from DSC and TGA thermograms are summarized in Table X, as supplementary info.)

3.2 Swelling tests of cryogels

The swelling behaviours of the prepared cryogels is very important in terms of their usability based on adsorption studies. Cryogels do not dissolve in the aqueous medium, but swell by holding water, depending on the degree of crosslinking and the hydrophilic property of the polymer matrix. Therefore, this privilege also applies to the synthesized cryogels for this study. At this stage of the study, the swelling properties of HEMA-based cryogels prepared by functioning with N-vinylformamide (VF) and N-vinylpyrrolidone (VP) were investigated by the addition of these comonomers to the structure. p(HEMA)-based cryogels have hydrophilic structures so that their ability to absorb large amounts of water. p(HEMA) cryogels have a mesh-like porous structure thanks to their crosslinking with N,N'-methylene(bisacrylamide). p(HEMA)-based cryogels show the ability to hold a high amount of water within this reticulated structure. The weight-based equilibrium swelling rates of prepared cryogels for this study were calculated as 8.69 g H_2O/g cryogel, 8.99 g H_2O/g cryogel and 8.83 g H_2O/g cryogel for p(HEMA), p(HEMA-VF) and p(HEMA-VP) cryogels, respectively. In other words, the percentage of swelling rates were measured as 869%, 899% and, 883% for p(HEMA), p(HEMA-VF) and, p(HEMA-VP), based cryogels respectively. As a result of the hydrophilic comonomers they contain p(HEMA-VF) and p(HEMA-VP) cryogels, the swelling and swelling rates are higher than the pure p(HEMA) cryogel. In addition, thanks to the large surface area and wider pore size range contained by the two new pHEMA-derived cryogels, it provides higher swelling values by allowing it to hold more water than pure p(HEMA) cryogel. Since p(HEMA-VF) and p(HEMA-VP) cryogels are more hydrophilic, they interact with more water molecules. It is very important that pore shape, size and pores are interconnected in terms of transporting nutrients, drugs or many different derivatives such as waste materials. In addition, pore size is very important for chemical molecules that will settle in cryogels to attach and reproduce there. Therefore, the porosity of the prepared cryogel is an easy-to-apply and fast method that can potentially give an idea for the usability of chemical release systems [54]. Also, the % porosity values for (p(HEMA): %75.47, p(HEMA-VF): %80.26, and p(HEMA-VP): %79.12) was calculated according to Eq. (2). The gelling efficiency is an indicator of the crosslinking quality of the polymers synthesized and therefore whether the monomers are effectively converted into polymers [10]. In this study, gelling efficiency rates (p(HEMA): %90, p(HEMA-VF): %88, and p(HEMA-VP): %86) of all cryogels are very close to each other. This result shows that the applied freezing regime and polymerization process is both reproducible and not affected by the presence of comonomers. The results for physicochemical properties for all cryogels are presented in Table 2.

The solubility parameter expressed by the symbol δ is known as the square root of the evaporation energy per unit of material. Thus, δ is closely related to the adhesion of the material or the force of attraction between the molecules that make up the material. A method that can be frequently applied for crosslinked polymers or that can be adapted to a partially crystalline material is based on evaluating the

Table 2 Physicochemical properties of all cryogels

Cryogel columns	Specific surface area (m^2/g)	Pore size diameter (μm)	Porosity (%)	Gelling efficiency (%)	Water uptake (gH_2O/g cryogel)
p(HEMA)	15.31	2–100	75.47	90	8.69
p(HEMA-VF)	16.99	2–100	80.26	88	8.93
p(HEMA-VP)	16.44	2–100	79.12	86	8.83

Table 3 Swelling behavior results of p(HEMA), p(HEMA-VF) and p(HEMA-VP) cryogels in various solvents

Solvent	δ (cal/cm^3)$^{1/2}$ [58]	% swelling ratio p(HEMA)	% swelling ratio p(HEMA-VF)	% swelling ratio p(HEMA-VP)
n-Hexane	7.3	275.68	241.44	308.90
Benzene	9.2	361.37	340.92	293.66
Chloroform	9.3	466.27	464.43	535.15
Acetone	9.9	488.82	519.37	529.50
Acetonitrile	11.9	245.46	171.43	126.96
DMF	12.1	912.66	836.07	505.68
Ethanol	12.7	746.27	784.43	755.15
DMSO	12.9	885.97	1012.13	850.96
Methanol	14.5	535.67	408.05	451.13
Water	23.4	868.80	898.40	882.60

maximum in swelling using a series of solvents of variable and known solubility parameters [55]. As clearly seen from Table 3, the swelling ratio of cryogels in different solvents, it is observed that there is an increasing tendency from non-polar organic solvents to solvents with a high polar character, such as from n-hexane to ethanol or water. This further enhanced the swelling capacity of its hydrophilic monomers, such as N-vinylformamide and N-vinylpyrrolidone, which are also incorporated as comonomers in cryogels of HEMA-based structure. Some studies on the swelling behavior of hydrogels in different solvents have recently been included in the literature [56, 57]. As far as is known, no such investigation has yet been carried out for cryogels. At this point, in this study, which will be a first in the literature, the highest swelling tendency of HEMA-based cryogels could be expected to be in water. However, as a result of the swelling test in DMSO, which is known as the solvent with the highest dielectric constant and polarity, it was calculated that p(HEMA-VF) cryogel has the highest swelling rate. For another interesting evidence that p(HEMA) cryogel has shown over 9 times greater swelling in DMF, which has the second one highest dielectric constant, and polarity solvent in this group. It is understood that HEMA-based cryogels can better swell in polar solvents. Swelling behavior of

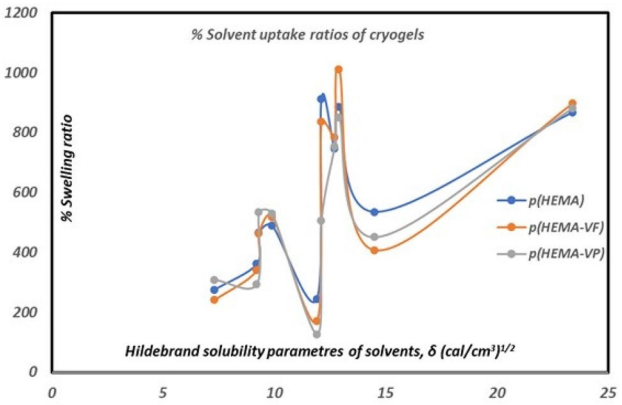

Fig. 6 % Solvent uptake ratios of cryogels (Color figure online)

cryogels in various solvents as % uptake ratios are presented in Fig. 6.

3.3 Chemical release behaviour of cryogels

The optical photographs of dye loaded cryogels and dye releases are presented in Fig. 7. MR was preferred as one of a model test compounds in release studies due to its very dark color in aqueous solutions and low biodegradability due to the presence of aromatic groups in its structure [59]. Cryogels are critical in biological applications due to their osmotic, chemical, and mechanical stability as well as being water-insoluble polymeric structures composed of hydrophilic copolymers and depending on the presence of the cross-linkers, in which they contain [60]. Furthermore, due to their macroporous structure, cryogels exhibit rapid swelling kinetics. As a result of these advantages, they are used as carrier molecules in the design of release systems for various drugs, proteins, peptides, and a variety of chemical compounds [61]. In this study, the release mechanism was based on swelling controlled systems, for which the controlled release occurs due to swelling of the polymer by taking water [62]. The swelling increases the elasticity of the polymer and provides the formation of large pores. Drug release from swellable polymers is based on the glassy-elastic transition of the polymer as a result of the solvent entering the polymer matrix. As soon as the solvent enters the polymer structure, the polymer swells and the glass

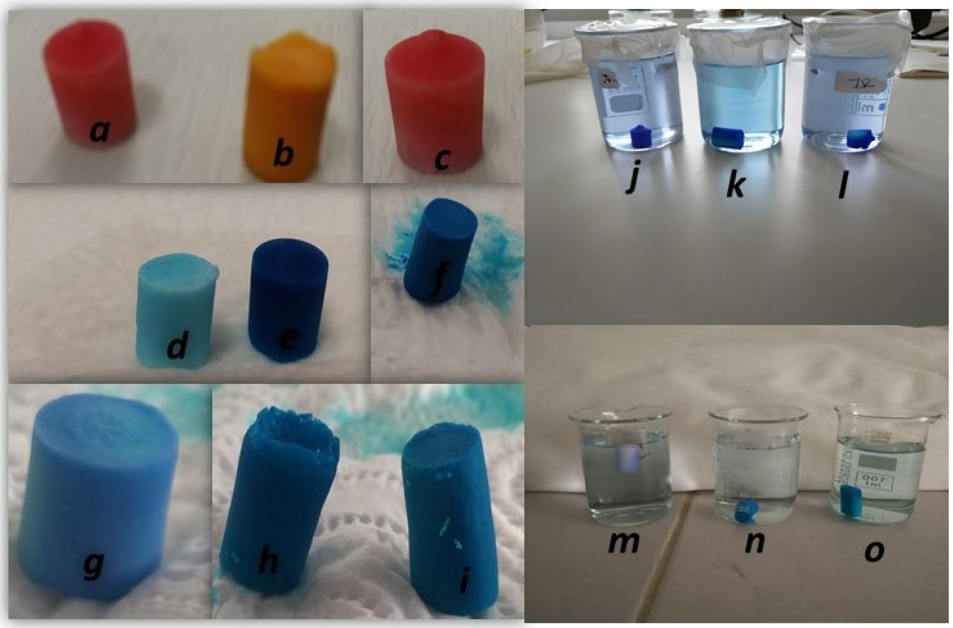

Fig. 7 Optical photographs for dye loaded-cryogels and dye releases process: **a** MR-adsorbed p(HEMA-VF) cryogel, **b** MR-adsorbed p(HEMA) cryogel, **c** MR-adsorbed p(HEMA-VP) cryogel, **d** MB-adsorbed p(HEMA) cryogel, **e** MB-adsorbed p(HEMA-VF) cryogel, **f** MB-adsorbed p(HEMA-VP) cryogel, **g** MG-adsorbed p(HEMA) cryogel, **h** MG-adsorbed p(HEMA-VF) cryogel, **i** MG-adsorbed p(HEMA-VP) cryogel, **j** MB-release from p(HEMA) cryogel, **k** MB-release from p(HEMA-VF) cryogel, **l** MB-release from p(HEMA-VP) cryogel, **m** MG-release from p(HEMA) cryogel, **n** MG-release from p(HEMA-VF) cryogel, **o** MG-release from p(HEMA-VP) cryogel (Color figure online)

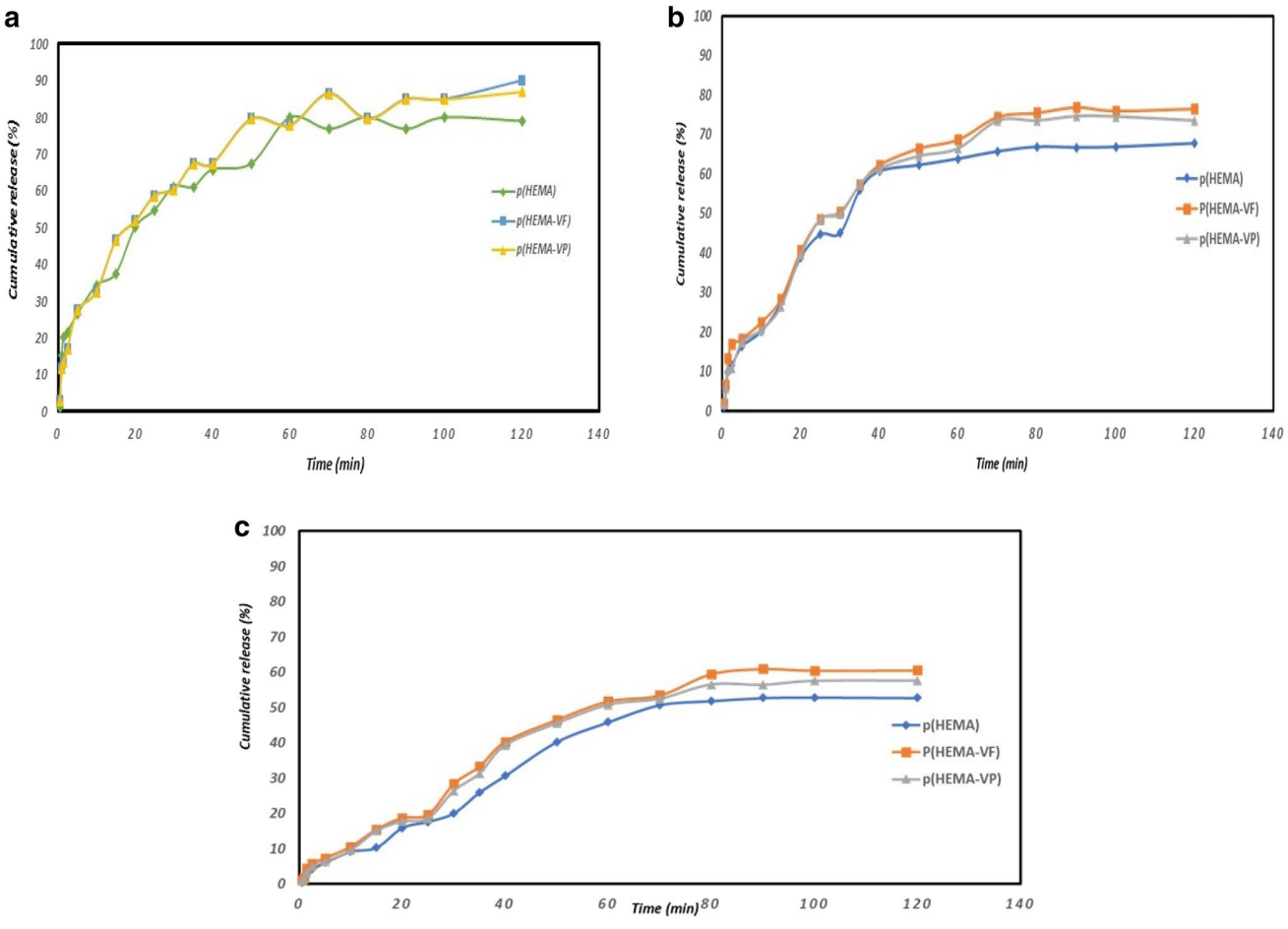

Fig. 8 Chemical release of dyes from p(HEMA), p(HEMA-VF) and p(HEMA-VP) cryogels as cumulative calculations: **a** (for MR from cryogels), **b** (for MB from cryogels), **c** (for MG from cryogels) (Color figure online)

transition temperature drops. Thus, the glassy polymeric structure becomes elastic and drug release begins. When we examine the chemical release behavior of cryogel samples in Fig. 8, we understand that all cryogels perform free release. During the first 25 min of release, p(HEMA-VF) and p(HEMA-VP) cryogels produced approximately 58.64% of MR's release, while pure p(HEMA) released 54.68%. The release rate reached 60% by the 30th minute. Generally, the cryogel samples exhibited similar release behavior, and p(HEMA-VF) and p(HEMA-VP) cryogels produced a total release of 89.98% and 86.64%, respectively, over a 120-min period. Also, pure p(HEMA) cryogel columns reached 80% as the maximum release level, which is lower than that of p(HEMA-VP) and p(HEMA-VF) cryogel columns. We can explain the release capacity of p(HEMA-VF) and p(HEMA-VP) cryogels to higher values compared to pure p(HEMA) cryogel. The hydrophilic character of p(HEMA-VF) and p(HEMA-VP) cryogels was increased compared to HEMA-based cryogels after the addition of N-vinylformamide and N-vinylpyrrolidone to HEMA-based cryogels as evidenced by the water uptake experiments. The release of chemical substances became easier and higher after the swelling with water after the change of the hydrophilic character of the cryogels showing free release behavior progressing with the swelling controlled system mechanism. MB is a water-soluble basic dye that is observed in dark colors and even in trace concentrations. The alkaline character of the p(HEMA-VF) and p(HEMA-VP) comonomers enabled these cryogels to have strong covalent interactions with MB. Since p(HEMA-VF) and p (HEMA-VP) cryogels strongly adsorb MB, the percent release of MB from these cryogels is higher than that of pure p(HEMA) cryogel. However, these results in Fig. 8b. has shown that it remains at a relatively low level compared to MR release from all HEMA-based cryogels. The release of MB from both p(HEMA-VF) and p (HEMA-VP) cryogel columns are delayed as a result of the strong alkaline interaction between comonomers of cryogels and MB. MG is alkaline-cationic dye, and it can be used as a pH indicator, which is green in the pH 2–3 range. However, it turns blue at pH values are greater than 3. [63]. Since distilled water was used as the solvent in order to prepare of MG solution, the color of the mixture turned blue in a short time. 60.58% MG was released from the p(HEMA-VF) cryogel after 120 min. Over the same period of time, this cumulative result was found to be 57.65% and 52.76% for p (HEMA-VP) and pure p(HEMA) cryogels, respectively. The acidic dye MR release occurs faster than MB and MG releases known as alkaline dyes. This result can be explained by the stronger covalent interaction of alkali monomers such as VF and VP in the p (HEMA) structure against dyes with similar character such as MB or MG.

Absorption of water from the environment in the polymeric gel system affects the dimensions, physicochemical properties and hence drug release kinetics of the system. Although there are many mathematical models that model drug release from swellable polymeric systems, a single model alone is not successful enough to predict all the experimental observations. Generalized empirical equations are frequently used in drug release, since even the most complex models do not provide the appropriate formula and require many solution techniques. In this study, the equation defined by Peppas, which is detailed in Eq. (4) and Eq. (5), are used in order to determine the release mechanism of cryogels. The relative effect of macromolecular relaxation on the drug delivery mechanism can be easily determined by modifying the experimental data to this equation. However, this equation can be applied for during the first 60% of the total drug release. "Eq. (5)." is used to describe the overall transport behavior of the solvent in the polymer and describes the type of diffusion mechanism depending on the value of ''n''. The basis of ''n'' is obtained by plotting the output of this equation on the logarithmic scale and calculating the linear slope and the correct slope. In Table 4, n and k values for released from cryogel columns containing different dyes are presented together with the regression coefficientsare. The 'n' release exponential, which determines the drug release mechanism, is calculated between 0.5 and 1 in all release studies. The value of 'n' between these values shows that the emission complies with the non-fickian theory according to the Power law. The release compliance with this law indicates that the system that controls dye release from the HEMA-based cryogel columns is a mixture of swelling and diffusion-controlled release. The 'k' value obtained from the power law and expressed as diffusion exponential has increased with the increase of the emission percentage cumulatively, in other words, the acceleration of the release.

Table 4 n, k and R^2 values for all dye released cryogels

Cryogel	n	k	R^2
MR released from p(HEMA)	0.5223	0.0481	0.978
MR released from p(HEMA-VF)	0.6557	0.0608	0.995
MR released from p(HEMA-VP)	0.5423	0.0581	0.986
MB released from p(HEMA)	0.5110	0.0461	0.965
MB released from p(HEMA-VF)	0.611	0.0592	0.987
MB released from p(HEMA-VP)	0.602	0.0543	0.974
MG released from p(HEMA)	0.507	0.0396	0.962
MG released from p(HEMA-VF)	0.555	0.0533	0.975
MG released from p(HEMA-VP)	0.513	0.0498	0.969

4 Conclusions

In this study, the synthesis and characterization of p(HEMA-VF) and p(HEMA-VP) cryogels containing N-VF and N-VP comonomers were performed for the first time in literature. Via DSC and TGA, it is shown that p(HEMA-VF) and p(HEMA-VP) have improved comparability as compared to pure HEMA-based cryogels. Due to hydrophilic character of the comonomers contained in p(HEMA-VF) and p(HEMA-VP) cryogels, the swelling properties in water are improved significantly. Thus, cryogels are hydrophilic polymers capable of absorbing large amounts of water and water-soluble analytes. As a result, it may provide a cell or tissue-like environment to function biologically or naturally [64]. Furthermore, it was found that the chemical stability or physical properties of cryogels in different character solvents did not deteriorate, while maintaining their swelling properties partially. Considering the experimental feedbacks and the mathematical models applied to these results, the chemical release performances of the synthesized cryogels may be preferred as alternative polymeric systems for future experimental studies based on drug release using as injectable cryogels.

Acknowledgements This work was supported financially by the Düzce University Research Fund (Grant Number 2019.05.03.1024).

References

1. T. Zhang, Z. Xu, H. Gui, Q. Guo, J. Mater. Chem. A **5**, 10161 (2017)
2. K.J. De France, F. Xu, T. Hoare, Adv. Healthc. Mater. **7**, 1700927 (2018)
3. M.M. Elsayed, J. Polym. Environ. **27**, 871 (2019)
4. L.L. Palmese, R.K. Thapa, M.O. Sullivan, K.L. Kiick, Curr. Opin. Chem. Eng. **24**, 143 (2019)
5. V. Baudron, P. Gurikov, I. Smirnova, S. Whitehouse, Gels **5**, 12 (2019)
6. T. Sedlačík, T. Nonoyama, H. Guo, R. Kiyama, T. Nakajima, Y. Takeda, T. Kurokawa, J.P. Gong, Chem. Mater. **32**, 8576 (2020)
7. M. Zinggeler, J.N. Schönberg, P.L. Fosso, T. Brandstetter, J. Rühe, A.C.S. Appl, Mater. Interfaces **9**, 12165 (2017)
8. E. Su, O. Okay, Polymer (Guildf). **178**, 121603 (2019)
9. M. Razavi, Y. Qiao, A.S. Thakor, J. Biomed. Mater. Res. Part A **107**, 2736 (2019)
10. V. Lozinsky, Gels **4**, 77 (2018)
11. K. Şarkaya, M. Bakhshpour, A. Denizli, Sep. Sci. Technol. **1**, 271 (2018)
12. V.I. Lozinsky, Adv. Polym. Sci. (2014). https://doi.org/10.1007/978-3-319-05846-7
13. I. Perçin, N. Idil, A. Denizli, Process Biochem. **80**, 181 (2019)
14. M.D. Stanescu, A. Sanislav, R.V. Ivanov, A. Hirtopeanu, V.I. Lozinsky, Appl. Biochem. Biotechnol. **165**, 1789 (2011)
15. M. Zhai, F. Ma, J. Li, B. Wan, N. Yu, J. Biomater. Sci. Polym. Ed. **29**, 1401 (2018)
16. D.F.A. Loghin, G. Biliuta, S. Coseri, E.S. Dragan, Int. J. Biol. Macromol. **96**, 589 (2017)
17. G. Uzunoğlu, D. Çimen, N. Bereli, K. Çetin, A. Denizli, J. Biomater. Sci. Polym. Ed. **30**, 1276 (2019)
18. G. Güven, S. Evli, M. Uygun, D.A. Uygun, J. Liq. Chromatogr. Relat. Technol. **42**, 537 (2019)
19. M. Mavlan, L. Uzun, J.P. Youngblood, Cellulose **7**, 1 (2020)
20. K. Şarkaya, M. Bakhshpour, A. Denizli, Sep. Sci. Technol. **54**, 2993 (2019)
21. K. Çetin, A. Denizli, Process Biochem. **79**, 174 (2019)
22. B. Dmitriy, J. Clean. Prod. **247**, 119089 (2020)
23. M. Çadırcı, K. Şarkaya, A. Allı, Mater. Sci. Semicond. Process. **119**, 105269 (2020)
24. R. Jirakunakorn, S. Khumngern, J. Choosang, P. Thavarungkul, P. Kanatharana, A. Numnuam, Microchem. J. **154**, 104624 (2020)
25. I. Guven, O. Gezici, M. Bayrakci, M. Morbidelli, J. Chromatogr. A **1558**, 59 (2018)
26. S.S. Suner, S. Demirci, B. Yetiskin, R. Fakhrullin, E. Naumenko, O. Okay, R.S. Ayyala, N. Sahiner, Int. J. Biol. Macromol. **130**, 627 (2019)
27. S.T. Koshy, D.K.Y. Zhang, J.M. Grolman, A.G. Stafford, D.J. Mooney, Acta Biomater. **65**, 36 (2018)
28. A.Z. Baimenov, D.A. Berillo, V.J. Inglezakis, J. Mol. Liq. **299**, 112134 (2020)
29. R. Yao, Z. Yao, J. Zhou, Mater. Lett. **176**, 199 (2016)
30. S. Pacelli, L. Di Muzio, P. Paolicelli, V. Fortunati, S. Petralito, J. Trilli, M.A. Casadei, *Int* (J. Biol, Macromol, 2020).
31. K. Çetin, H. Alkan, N. Bereli, A. Denizli, J. Macromol. Sci. Part A **54**, 502 (2017)
32. J. Li, Y. Wang, L. Zhang, Z. Xu, H. Dai, W. Wu, A.C.S. Sustain, Chem. Eng. **7**, 6381 (2019)
33. G.G. de Lima, F. Traon, E. Moal, M. Canillas, M.A. Rodriguez, H.O. McCarthy, N. Dunne, D.M. Devine, M.J.D. Nugent, Polym. Compos. **39**, E210 (2018)
34. H. Zhao, J. Gao, R. Liu, S. Zhao, Carbohydr. Res. **428**, 79 (2016)
35. X. Zhou, J. Wang, J. Nie, B. Du, Polym. J. **48**, 431 (2016)
36. H. Huang, L. Hou, F. Zhu, J. Li, M. Xu, RSC Adv. **8**, 9334 (2018)
37. B.L. Abraham, E.S. Toriki, N.J. Tucker, B.L. Nilsson, J. Mater. Chem. B **8**, 6366 (2020)
38. N.I. Gorshkov, I.E. Alekseev, A.E. Miroslavov, A.Y. Murko, A.A. Lumpov, V.D. Krasikov, D.N. Suglobov, Int. J. Polym. Anal. Charact. **23**, 290 (2018)
39. N.I. Gorshkov, A.E. Miroslavov, I.E. Alekseev, A.A. Lumpov, A.Y. Murko, I.I. Gavrilova, N.N. Saprykina, M.A. Bezrukova, A.I. Kipper, V.D. Krasikov, D.N. Suglobov, M.Y. Tyupina, E.F. Panarin, J. Label. Compd. Radiopharm. **60**, 302 (2017)
40. H. Peng, X. Huang, A. Melle, M. Karperien, A. Pich, J. Colloid Interface Sci. **540**, 612 (2019)
41. M. Yue, K. Imai, Y. Miura, Y. Hoshino, Polym. J. **49**, 601 (2017)
42. O.I. Timaeva, N.A. Arkharova, A.S. Orekhov, V.V. Klechkovskaya, S.P. Mulakov, G.M. Kuz'micheva, I.I. Pashkin, Polymer Guildf. **186**, 122079 (2020)
43. P. Sheikholeslami, B. Muirhead, D.S.H. Baek, H. Wang, X. Zhao, D. Sivakumaran, S. Boyd, H. Sheardown, T. Hoare, Exp. Eye Res. **137**, 18 (2015)
44. H. Ajiro, K. Kan, M. Akashi, J. Nanosci. Nanotechnol. **17**, 837 (2017)
45. J. Long, B. Liang, S. Li, and zhenbin Chen. J. Sep. Sci. **40**, 4847 (2017)
46. K. Şarkaya, A. Demir, Polym. Bull. (2019). https://doi.org/10.1007/s00289-018-2657-7
47. L. Shan, Y. Gao, Y. Zhang, W. Yu, Y. Yang, S. Shen, S. Zhang, L. Zhu, L. Xu, B. Tian, J. Yun, Ind. Eng. Chem. Res. **55**, 7655 (2016)
48. J. Siepmann, N.A. Peppas, Int. J. Pharm. **418**, 6 (2011)

49. I.Y. Wu, S. Bala, N. Škalko-Basnet, M.P. di Cagno, Eur. J. Pharm. Sci. **138**, 105026 (2019)
50. N. Sahiner, Polym. Adv. Technol. **29**, 2184 (2018)
51. E. Jain, A. Damania, A.K. Shakya, A. Kumar, S.K. Sarin, A. Kumar, Colloids Surfaces B Biointerfaces **136**, 761 (2015)
52. D. Pamfil, C. Schick, C. Vasile, Ind. Eng. Chem. Res. **53**, 11239 (2014)
53. B.D. Fecchio, S.R. Valandro, M.G. Neumann, C.C.S. Cavalheiro, J. Braz. Chem. Soc. **27**, 278 (2016)
54. I.E. Raschip, N. Fifere, C.D. Varganici, M.V. Dinu, Int. J. Biol. Macromol. **156**, 608 (2020)
55. S.S. Liu, X.P. Li, P.J. Qi, Z.J. Song, Z. Zhang, K. Wang, G.X. Qiu, G.Y. Liu, Polym. Test. **81**, 106170 (2020)
56. M.V. Martinez, M. Molina, C.A. Barbero, J. Phys. Chem. B **122**, 9038 (2018)
57. M.V. Martinez, M.A. Molina, S.B. Abel, C.A. Barbero, MRS Adv. **3**, 3735–3740 (2018)
58. J. Sameni, S. Krigstin, M. Sain, Acetylation & Lignin Solubility **12**, 1548 (2017)
59. İ Şener, K. Şarkaya, Süleyman Demirel Üniversitesi Fen Edeb. Fakültesi Fen Derg. **8**, 175 (2013)
60. K. Çetin, A. Denizli, Colloids Surfaces B Biointerfaces **126**, 401 (2015)
61. P. Öncel, K. Çetin, A.A. Topçu, H. Yavuz, A. Denizli, J. Biomater. Sci. Polym. Ed. **28**, 519 (2017)
62. M. Bakhshpour, H. Yavuz, A. Denizli, Artif Cells Nanomedicine Biotechnol. **46**, 946 (2018)
63. P. Sharma, B.K. Saikia, M.R. Das, Colloids Surfaces A Physicochem. Eng. Asp. **457**, 125 (2014)
64. M.V. Konovalova, P.A. Markov, E.A. Durnev, D.V. Kurek, S.V. Popov, V.P. Varlamov, J. Biomed. Mater. Res. Part A **105**, 547 (2017)